Available online at www.sciencedirect.com
ScienceDirect
Computers and Mathematics with Applications 55 (2008) 1424–1432
An International Journal
computers & mathematics
with applications
www.elsevier.com/locate/camwa

A simple lattice Boltzmann scheme for combustion simulation

Sheng Chen[a,*], Zhaohui Liu[b], Zhiwei Tian[b], Baochang Shi[b], Chuguang Zheng[b]

[a] *National Technology Center, Wuhan Iron and Steel (Group) Company, Wuhan 430080, China*
[b] *State Key Laboratory of Coal Combustion, Huazhong University of Science and Technology, Wuhan 430074, China*

Abstract

A simple lattice Boltzmann model is developed for two-dimensional combustion simulations. In this model the time step and the fluid particle speed can be adjusted dynamically, depending on the "particle characteristic temperature". The algorithm is still a simple process of hopping from one grid point to the next, the same as the standard lattice Boltzmann method. Therefore the outstanding advantages of the standard lattice Boltzmann method are retained in this model besides better numerical stability. Excellent agreement between the present results and other numerical or experimental data shows that this scheme is an efficient numerical method for practical combustion simulations.

Keywords: Lattice Boltzmann method; Combustion; Low Mach number

1. Introduction

The process of combustion is highly complex. It involves fluid mechanical processes such as turbulent mixing and heat transfer but also other processes such as radiation and chemistry. The fact that the combustion involves these very different processes makes it not only a highly multi-disciplinary topic for research, but also a highly challenging one. For this reason the scientific problem of combustion has been nominated as one of the "Grand Challenges" to be solved when a Tera-flops computer becomes available, and this is the background of the project that we propose here.

Recently, the lattice Boltzmann method (LBM) has emerged as a promising alternative to solve various challenging flow problems [1–4]. These brilliant achievements benefit from its inherent outstanding advantages: simple numerical codes, easy parallel implementations and clear physical pictures, which let the LBM be more suitable for the current trend of massive computation and more easily solve some problems that are difficult in conventional numerical methods. However, compared with the so great success in multi-phase flows, porous media flows, magnetic flows, particulate suspensions and so on, the prospect of applying the LBM to combustion is not yet entirely clear, even though there has been a continuous endeavor in this area [5–11]. To the best of our knowledge, the latest published paper in which the LBM was applied to combustion simulation belongs to Yamamoto [10] and Yu [11]. In Ref. [10] the author simulated diffusion flames with turbulence based on a double-distribution-function LBM model proposed

* Corresponding author.
E-mail addresses: isdongyue@163.com (S. Chen), zliu@mail.hust.edu.cn (Z. Liu).

0898-1221/$ - see front matter © 2007 Elsevier Ltd. All rights reserved.
doi:10.1016/j.camwa.2007.08.020

in his previous work [9]. The main feature of this scheme is that the temperature field does not affect the flow field. The simplification adopted by Yamamoto et al. is very apt to make anyone recall the work done by Succi et al. who are the pioneers to extend the LBM to the solution of combustion problems [5]. In the limiting case of irreversible infinite fast chemistry reactions and "cold" flames with weak heat release Succi et al. have described the reactive flow dynamics in two dimensions with the 24 speeds FCHC model including two passive scalars as mixture fraction of the fuel and temperature. In spite of the significant differences in their appearances and technical details, these models share one common shortcoming in their constructions of the LBM model for combustion simulations: they both cannot handle variable density, which is an important factor in combustion problems. In most practical reacting flows, the flow, temperature and concentration fields are coupled through the variable density which is allowed to respond to temperature changes over a significant dynamical range of values [7]. It is not surprising that those numerical results will deviate from the real physical phenomena, as the authors showed in their work [5,9,10]. From our point of view, these models can fall into a same category which is referred to as "non-coupled" lattice Boltzmann (NCLB) model in this paper. The limitation of this approach is obvious and we shall have no further discussion about it.

What is worthy to be emphasized particularly is the contribution made by Filippova et al. [6–8] who introduced the low Mach number approximation into the LBM to simulate combustion. The low Mach number approximation is reasonable in most practical combustion processes because the acoustic influence on reaction problems is not of interest in such cases [7]. In such combustion, reactive flows at low speeds are characterized by low Mach numbers ($M \ll 1$) but with significant changes in the density due to temperature changes by chemical reactions. Consequently the hydrodynamics equations for this kind of reacting flows are the variable density Navier–Stokes equations instead of the full compressible Navier–Stokes equations [12]. Because of the differences between the macroscopic target equations, Filippova et al. could construct their model based on the pressure-like distribution function developed for incompressible isothermal flows instead of the standard particle density distribution function. The second difference between the model proposed by Filippova et al. and the NCLB is that their model is a hybrid scheme instead of the pure LBM scheme, in which the flow simulation is decoupled from the solution of the temperature/species equations. Specifically, the flow simulation is accomplished by using the LBM, while the temperature/species equations are solved by using finite-difference schemes. The notable improvement in this hybrid scheme is that it can handle the variable density. But, there still exist some shortcomings in this scheme. On one hand, the simplicity property of the pure LBM scheme, which is always an important aspect of the LBM development [13], has been lost [9]. On the other hand, one must pay additional special attention to handle its pressure-like term at boundaries [7]. In Refs. [7,8] this hybrid scheme is verified only through artificial reactions with the maximal temperature ratio less than 4. But, such small temperature ratios cannot satisfy the actual needs of most practical combustion simulations [9].

In this paper, a novel LBM model for combustion simulations, which follows the line of Filippova et al., is proposed to overcome the above shortcomings. Different to the NCLB, this model is coupled; different to the hybrid scheme, this model is strictly pure LBM style (i.e., we solve the flow, temperature, and concentration fields using LBM schemes only). Besides the intrinsic advantages of the standard LBM, this model has better numerical stability and can bear a higher temperature ratio.

2. Low Mach number approximation of Navier–Stokes equations (LMNA)

The low Mach number approximation of Navier–Stokes equations are derived from the full set of conservation equations for mass, momentum, energy and mass fractions of species by expanding the normalized variables in a series of square Mach numbers and neglecting terms of second order in Mach number compared to dominant terms [14–16]:

$$\partial_t \rho + \nabla_\alpha \rho u_\alpha = 0, \tag{1}$$

$$\partial_t \rho u_\alpha + \nabla_\beta \rho u_\alpha u_\beta = -\nabla_\alpha p_1 + \nabla_\beta \mu(\nabla_\alpha u_\beta + \nabla_\beta u_\alpha), \tag{2}$$

$$\rho C_p(\partial_t T + u_\alpha \nabla_\alpha T) = \nabla_\alpha C_p \kappa \rho \nabla_\alpha T + \sum_{i=1}^{N} h_i \omega_i + \partial_t p_0, \tag{3}$$

$$\rho(\partial_t Y_i + u_\alpha \nabla_\alpha Y_i) = \nabla_\alpha D_i \rho \nabla_\alpha Y_i + \omega_i, \quad i = 1, \ldots, N-1$$

$$\sum_{i=1}^{N} Y_i = 1. \tag{4}$$

The main assumption in the LMNA is that the pressure P can split in two parts: the "thermodynamic pressure" p_0 and the "hydrodynamic pressure" p_1. p_0 can only be a function of time. In an open system, p_0 is a constant with an arbitrary value, say atmospheric pressure, therefore the last term in the temperature Eq. (3) vanishes. The density ρ of the mixture can be got by

$$\rho = \frac{p_0 \overline{W}}{RT}, \tag{5}$$

where $\mathbf{u}$, T and μ are the density, velocity, temperature and dynamic viscosity of the mixture. ω_i and h_i are the rate of production and heat of formation of the ith species respectively. In addition, R is the universal gas constant and $\overline{W}$ is the mean molecular weight of the mixture given by

$$\overline{W} = 1 \Big/ \sum_{i=1}^{N} \frac{Y_i}{W_i}. \tag{6}$$

W_i is the molecular weight of the ith species. Note that, in the present study, the subscripts α and β represent Cartesian coordinates and the summation convention is applied to these subscripts.

3. Lattice Boltzmann scheme for Low Mach number combustion

Our model is based on the idea of the double-distribution-function model proposed by Shan et al. [17], which originally was developed to simulate multi-phase flows. Then it was extended to thermal flows [18]. Later Yamamoto et al. employed the double-distribution-function model to simulate combustion [9,10]. Its main feature is that the flow, temperature, and species fields are represented by two sets of distribution functions: one simulates the Navier–Stokes equations, and the other simulates the advection-diffusion equation satisfied by the temperature/concentration fields. Compared to the multi-speed model [19], such model has the advantage of simplicity and can easily handle an arbitrary value of the Prandtl number besides better numerical stability. Following we take the 2D 9-speed model for an example, whose discrete velocities $\mathbf{e}_k$ are 0 for the rest-particle, $(\cos[(k-1)\pi/2], \sin[(k-1)\pi/2])$ for the horizontal and vertical links and $(\cos[(k-5)\pi/2+\pi/4], \sin[(k-5)\pi/2+\pi/4])$ for the diagonal links.

3.1. Flow field

The evolution equation for the flow field is improved from the model proposed by Guo et al. [20], described by

$$g_k(\mathbf{x} + c\mathbf{e}_k \Delta t, t + \Delta t) - g_k(\mathbf{x}, t) = -\tau_u^{-1}[g_k(\mathbf{x}, t) - g_k^{(\mathrm{eq})}(\mathbf{x}, t)] \tag{7}$$

where $c = \Delta x/\Delta t$ is the fluid particle speed. Δx, Δt and τ_u are the lattice grid spacing, the time step and the dimensionless relaxation time for the flow field respectively. $g_k(\mathbf{x}, t)$ is the distribution function at node x and time t with velocity $\mathbf{e}_k$, and $g_k^{(\mathrm{eq})}(\mathbf{x}, t)$ is the corresponding equilibrium distribution. The equilibrium distribution in our model is defined by

$$g_k^{(\mathrm{eq})} = \chi_k + \rho s_k(\mathbf{u}) \tag{8}$$

where $\chi_0 = \rho - 4\sigma p_1/c^2$, $\chi_k = \lambda p_1/c^2$ for $k = 1, 2, 3, 4$, and $\chi_k = \gamma p_1/c^2$ for $k = 5, 6, 7, 8$. Parameters σ, λ, γ satisfy $\lambda + \gamma = \sigma$, $\lambda + 2\gamma = 0.5$ and

$$s_k(\mathbf{u}) = \omega_k \left[3\frac{(\mathbf{e}_k \cdot \mathbf{u})}{c} + \frac{9}{2}\frac{(\mathbf{e}_k \cdot \mathbf{u})^2}{c^2} - \frac{3}{2}\frac{|\mathbf{u}|^2}{c^2} \right]. \tag{9}$$

The weights $\omega_0 = 4/9$, $\omega_k = 1/9$ $(k = 1, 2, 3, 4)$ and $\omega_k = 1/36$ $(k = 5, 6, 7, 8)$.

The kinematic viscosity is determined by

$$\nu = \frac{2\tau_u - 1}{6} c^2 \Delta t. \tag{10}$$

The density momentum and hydrodynamic pressure are given by

$$\rho \mathbf{u} = \sum_{k\geq 0} c\mathbf{e}_k g_k, \qquad p_1 = \frac{c^2}{4\sigma}\left[\sum_{k\neq 0} g_k + \rho s_0(\mathbf{u})\right]. \tag{11}$$

An interesting aspect of this model is that the value of density of the mixture is not obtained explicitly through the evolution equation (7). The same as in the hybrid scheme proposed by Filippova et al., in this model, at every new time step we obtain the new value of density by

$$\rho^{n+1} = \frac{\rho^n T^n \overline{W}^{n+1}}{T^{n+1}\overline{W}^n} = \frac{\rho_0 T_0 \overline{W}^{n+1}}{T^{n+1}\overline{W}_0} \tag{12}$$

according to the assumption of the LMNA (i.e., Eq. (5)), where $\overline{W}_0$ is the mean molecular weight of the mixture at the state ρ_0, T_0. Note that here and below the superscript n refers to the current time level and $n+1$ the next one. And in absence of temperature gradients, this model reduces to an incompressible model for isothermal flows [20], which agrees with the assumption of LMNA.

For the temperature dependent viscosity μ, we assume that

$$\frac{\mu}{\mu_0} = \sqrt{\frac{T}{T_0}}. \tag{13}$$

The reference viscosity $\mu_0 = \mu(T = T_0)$ is directly related to the Reynolds number Re by

$$Re = \rho_0 u_0 L_0/\mu_0. \tag{14}$$

T_0, L_0 and ρ_0 are reference values of temperature, length and density.

Through the Chapman–Enskog procedure, macrodynamical equations Eqs. (1) and (2) can be derived from above evolving equations. The detailed derivation could be found in Ref. [21].

3.2. Temperature and species fields

As above mentioned, the evolution equations for the temperature and species fields have the same form

$$f_{S,k}(\mathbf{x} + c\mathbf{e}_k\Delta t, t + \Delta t) - f_{S,k}(\mathbf{x}, t) = -\tau_S^{-1}[f_{S,k}(\mathbf{x}, t) - f_{S,k}^{(\mathrm{eq})}(\mathbf{x}, t)] + \omega_k Q_S \Delta t \tag{15}$$

where

$$f_{S,k}^{(\mathrm{eq})} = \omega_k S\left[1 + 3\frac{(\mathbf{e}_k\cdot\mathbf{u})}{c} + \frac{9}{2}\frac{(\mathbf{e}_k\cdot\mathbf{u})^2}{c^2} - \frac{3}{2}\frac{|\mathbf{u}|^2}{c^2}\right]. \tag{16}$$

The symbol S represents the species field of the ith species or the temperature field (i.e., $S = Y_i$, T). In Eq. (15) τ_S is the dimensionless relaxation time for S and Q_S is the source term due to chemical reactions. In LB calculation, Q_S is given by the similarity in non-dimensional equations of temperature and species fields. The temperature, T, and the mass fraction of species i, Y_i, are obtained in terms of the distribution function by

$$T = \sum_k f_{T,k}. \tag{17}$$

$$Y_i = \sum_k f_{Y_i,k}. \tag{18}$$

The thermal diffusivity, κ, and diffusion coefficient, D_i, are given by

$$\kappa = \frac{2\tau_T - 1}{6}c^2\Delta t. \tag{19}$$

$$D_i = \frac{2\tau_{Y_i} - 1}{6}c^2\Delta t. \tag{20}$$

3.3. Particle characteristic temperature

The foremost characteristic of our scheme is that the fluid particle speed can be adjusted dynamically, depending on the "particle characteristic temperature", for the purpose of the numerical stability. If the fluid particle speed is a constant value during combustion simulations, the limitation $O(|\mathbf{u}|/c) \sim O(M) \ll 1$ and the Courant–Friedricks–Lewey condition perhaps would not be satisfied due to the increasing value of local velocity. In some existing schemes the fluid particle speed depends on the local temperature T [22]. In such schemes, the calculated distributions at the next time step may not reside on the grid nodes because the fluid particle speed on different grid nodes may have different value. A reconstruction step is necessary to compute the information on the grid nodes; therefore interpolations have to be used, but which will introduce undesirable numerical artifacts [22].

In order to avoid the reconstruction step as well as to assure the numerical stability, we introduce a concept, "particle characteristic temperature", into our model. The temperature that determines the value of the fluid particle speed is called the "particle characteristic temperature" in this paper. For example, in combustion, the maximum temperature $T_{\max}$ of the mixture can serve as the "particle characteristic temperature". The fluid particle speed c^n is allowed to respond to $T^n_{\max}$ changes, i.e.,

$$\frac{c^n}{c_0} = \sqrt{\frac{T^n_{\max}}{T_0}} \tag{21}$$

c_0 is the reference value of the fluid particle speed at the temperature T_0. Therefore at time n the value of the fluid particle speed on different grid nodes can be the same.

In order to guarantee the algorithm to be a simple process of hopping from one grid point to the next, the same as the standard LBM, the particle speed c^n, the time step Δt^n, and the lattice grid spacing Δx must satisfy the following relationship

$$\Delta x = c^n \Delta t^n. \tag{22}$$

Because Δx is constant when the grid number has been determined, therefore now Δt^n has to vary at every iterative step, according to Eq. (22). It must be emphasized that in all existing lattice Boltzmann schemes Δt^n cannot be adjusted dynamically, which is the main reason that hampers the numerical stability in combustion. It is well-known that in conventional numerical methods, Δt^n can be adjusted freely to assure numerical stabilities [12]. Though the LMNA can filter out them when the whole system approaches to the steady state, the high frequency pressure waves generated at the forepart of ignition, will hamper numerical stabilities. This phenomenon, named as "overshoot", is well-known in combustion simulations by direct numerical simulations (DNS). In DNS, this difficulty can be overcome easily by adjusting Δt^n. Considering the fact that the LBM starts with the kinetic theory and has been derived to conserve high-order isotropy, the LBM should be more sensitive than conventional methods in capturing pressure waves [23], Δt^n also must be adjusted reasonably. But surprisingly, previous studies prefer to spend so great costs on such complicated models rather than try to adjust Δt^n. The idea that the fluid particle speed on different grid nodes can be adjusted at different iterative steps, but within each iterative step it has a uniform value, which depends on the "particle characteristic temperature", comes from He et al. [24]. In their work the fluid particle speed is proportional to $\sqrt{T_{av}}$ to avoid the reconstruction step, where T_{av} is the average temperature of the thermal flow. But, Δt^n is still kept a constant value in their model.

4. Results and discussions

To evaluate the performance of the present model, we simulated the so-called "counter-flow" premixed propane-air flame proposed by Yamamoto et al. [9], which is a benchmark test in the combustion science. Fig. 1 illustrates the computational domain and boundary conditions of such case. Two-dimensional rectangular coordinates are used. Two parallel stationary walls are located at $y = \pm L$. The combustible mixture is uniformly ejected from the top and bottom walls, and it reacts in the reaction zone. Then, the twin stagnation flames are formed in this counter flow. The burned gas flows outward along the x-direction.

In our simulation, the reaction is expressed with an over-all single step reaction [9]

$$C_3H_8 + 5O_2 \rightarrow 3CO_2 + 4H_2O$$

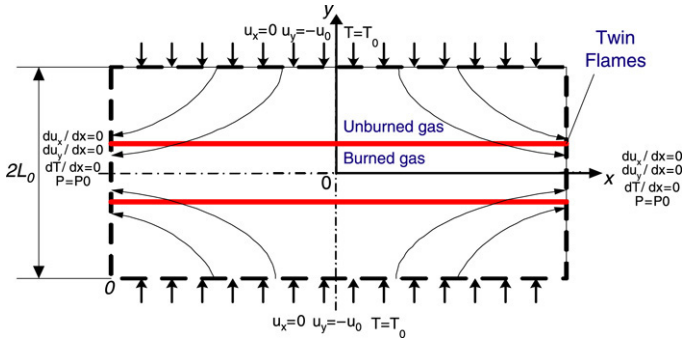

Fig. 1. Computational domain and boundary conditions.

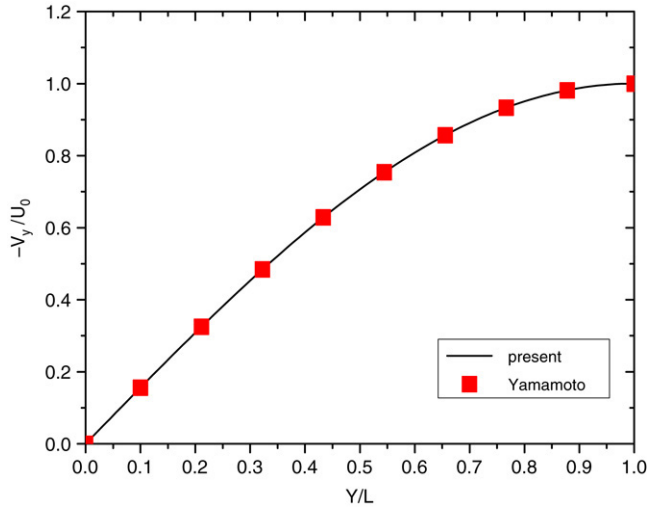

Fig. 2. Distributions of y-direction velocity u_y of the non-reactive flow, $x = 0$, $y \geq 0$.

with the over-all reaction rate ω_{ov} (mol/(m^3 s))

$$\omega_{ov} = k_{ov}\rho^2 \frac{Y_{C_3H_8}}{W_{C_3H_8}} \frac{Y_{O_2}}{W_{O_2}} \exp(-E/RT). \tag{23}$$

The reaction coefficient, k_{ov}, and the effective activation energy, E, are 9.9×10^{13} (cm^3/(mol s)) and 30 (kcal/mol) respectively. The universal gas constant, R, is 8.315 (J/(mol K)).

The mass rate of production for species i (kg/m^3 s) appearing in the conservation equation of species is

$$\omega_i = a_i \cdot W_i \cdot \omega_{ov}. \tag{24}$$

Stoichiometric coefficients, a_i, are $a_{C_3H_8} = -1$, $a_{O_2} = -5$, $a_{CO_2} = 3$, and $a_{H_2O} = 4$, respectively. The ambient temperature $T_0 = 300$ (K).

The equivalence ratio ϕ is obtained by

$$\phi = \frac{Y_{C_3H_8}/(1 - Y_{C_3H_8})}{0.0642}. \tag{25}$$

In LB calculation, the velocity at the wall is 0.1. The pressure at the outlet is 1/3. The initial density and the ambient temperature both are 1.

We first simulate the non-reactive case. The distributions of y-direction velocity u_y is shown in Fig. 2, together with the results obtained by the model proposed by Yamamoto et al. [9]. One can see that in this case the numerical results obtained by these two pure lattice Boltzmann models agree very well.

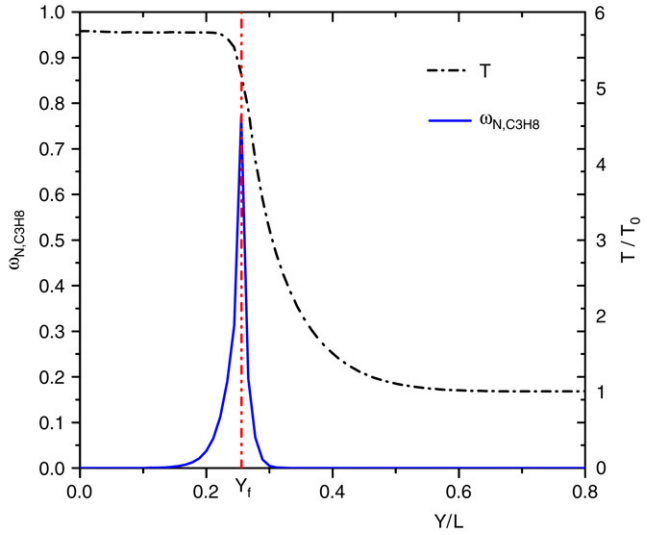

Fig. 3. Distributions of temperature and mass rate of production for propane, $x = 0$, $y \geq 0$.

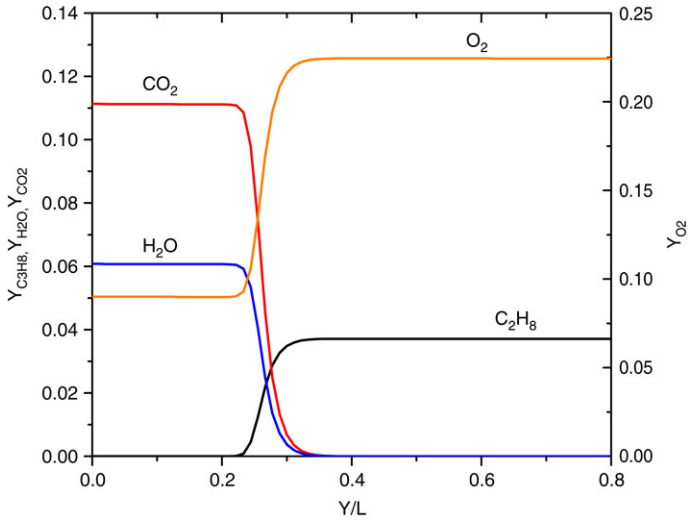

Fig. 4. Distributions of mass fraction of species, $x = 0$, $y \geq 0$.

Then a heat source is placed with high temperature to ignite the mixture. The unburned gas is ejected from the porous wall, and reacts in the flame zone, and finally it becomes burned gas. The temperature is almost constant along the x-axis. Figs. 3 and 4 show the temperature and concentration distributions at $x = 0$, $y \geq 0$ when the reactive flow achieves the steady state. The mass rate of production for propane ω_{N,C_3H_8} is also shown. The equivalence ratio is $\phi = 0.6$. One can see that, as the center is approached, the temperature starts to increase at $y/L \simeq 0.6$, and steeply increases at $y/L \simeq 0.2-0.3$. The reaction zone is located in this region, where the large heat release occurs to cause the temperature increase. Then, temperature becomes constant in the burned gas region. Though there is a long preheated zone, the reactants, C_3H_8 and O_2, do not decrease obviously until temperature rises to about 2.58 ($y/L \simeq 0.3$) (note that the kindling temperature of propane T_k is 766.48–822.05 (K), namely $T_k/T_0 \simeq 2.56$–2.74), then react in the reaction zone to form the products, CO_2 and H_2O. The fine structure of counter-flow flame is observed. Y_f is the flame stagnation position where ω_{N,C_3H_8} reaches its peak value.

Fig. 5 shows the distributions of y-direction velocity u_y of the reactive flow. One can see that in the present model the phenomenon that the velocity is accelerated due to the flow expansion caused by the increase in temperature can be

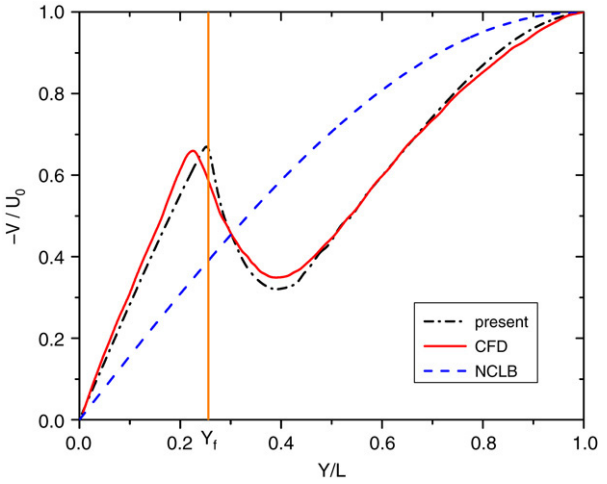

Fig. 5. Distributions of velocity of u_y, mass rate of production for propane, $x = 0$, $y \geq 0$.

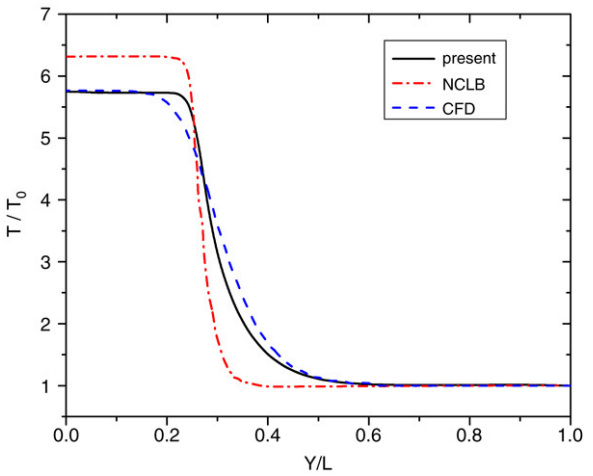

Fig. 6. Distributions of temperature.

captured exactly: at the flame stagnation position Y_f where the flame propagation speed $u_f = 0$, we can find the local flow velocity u_y (where $u_x = 0$) approximates to the burning velocity S_L. It agrees very well with the relationship $S_L = u_y - u_f$ because along this line ($x = 0$) it can be approximated to a one-dimensional problem [9]. Therefore, compared with the temperature field obtained by Yamamoto's model (referred by NCLB), the high temperature region obtained by the present model is wider, with lower maximum temperature, which agrees very well with the results obtained by conventional compressible finite-difference method (referred by CFD), as Fig. 6 shows. From Fig. 6, one can see that the present coupled model still performs very well even with a higher maximum temperature ratio which approaches 6.

In order to illustrate the numerical stability improvement more clearly, Fig. 7 only plots oscillations of the maximum temperature in the early stage after ignition. It is very clear that the maximum temperature will sharply increase in a minute and then decrease slowly. In conventional numerical methods, in order to assure numerical stabilities, one must adjust the time step during this period to guarantee the heat of formation due to chemical reactions is released into the mixture relatively slowly, otherwise the numerical results will diverge. In our model the fluid particle speed changes depending on the maximum temperature, therefore the time step will firstly decrease and then increase slowly. The variation tendency of time step in our model is consistent with that in conventional numerical methods. Consequently, we can assure the numerical stability besides the numerical efficiency. If the traditional LB

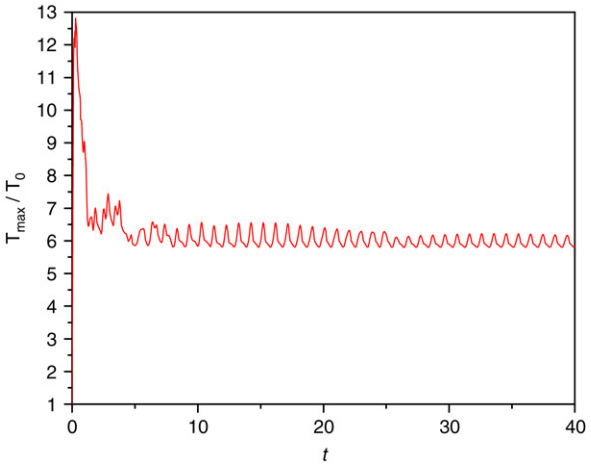

Fig. 7. Oscillations of the maximum temperature after ignition.

model is used without adjusting Δt^n dynamically, the numerical results will diverge before the maximum temperature reaches the peak value (the peak value is about 13 at $t \approx 0.31043$).

5. Conclusion

A novel coupled lattice Boltzmann model is proposed for two-dimensional low Mach number combustion simulations. In this model the time step and the fluid particle speed can be adjusted reasonably and the algorithm still is a simple process of hopping from one grid point to the next. This model has the following good features. It does not include any gradient term in the evolution equations, boundary condition can be easily implemented, and it preserves the simplicity of the standard LBM.

Acknowledgment

This work was partially supported by the Program for New Century Excellent Talents in University, Ministry of Education, China.

References

[1] R. Benzi, S. Succi, M. Vergassola, Phys. Rep. 222 (1992) 145.
[2] Y. Qian, S. Succi, S. Orszag, Annu. Rev. Comp. Phys. 3 (1995) 195.
[3] S. Chen, G. Doolen, Annu. Rev. Fluid Mech. 30 (1998) 329.
[4] D. Yu, R. Mei, L.S. Luo, W. Shyy, Prog. Aeosp. Sci. 39 (2003) 329.
[5] S. Succi, G. Bella, F. Papetti, J. Sci. Comput. 12 (1997) 395.
[6] O. Filippova, D. Hanel, Internat. J. Modern Phys. C 9 (1998) 1439.
[7] O. Filippova, D. Hanel, J. Comput. Phys. 158 (2000) 139.
[8] O. Filippova, D. Hanel, Comput. Phys. Comm. 129 (2000) 267.
[9] K. Yamamoto, X. He, Gary D. Doolen, J. Stat. Phys. 107 (2002) 367.
[10] K. Yamamoto, Internat. J. Modern Phys. B 17 (2003) 197.
[11] H. Yu, S. Girimaji, L.S. Luo, Int. J. Comput. Eng. Sci. 3 (2002) 73.
[12] N. Peters, Turbulent Combustion, Cambridge University Press, Cambridge, 2000.
[13] Y. Peng, C. Shu, Y.T. Chew, Phys. Rev. E 68 (2003) 026701.
[14] G.J. Sivashinsky, Acta Astronaut. 6 (1979) 631.
[15] A.G. Tomboulides, J.C.Y. Lee, S.A. Orszag, J. Sci. Comput. 12 (1997) 139.
[16] B.J. Boersma, Direct simulation of a jet diffusion flame, Annual Research Briefs, Stanford University, 1998.
[17] X.W. Shan, H.D. Chen, Phys. Rev. E 47 (1993) 1815.
[18] X.W. Shan, Phys. Rev. E 55 (1997) 2780.
[19] F.J. Alexander, S. Chen, J.D. Sterling, Phys. Rev. E 47 (1993) R2249.
[20] Z.L. Guo, B.C. Shi, N.C. Wang, J. Comput. Phys. 165 (2000) 288.
[21] S. Chen, Ph.D. Thesis, Huazhong University of Science and Technology, 2005.
[22] P. Lallemand, L.S. Luo, Phys. Rev. E 68 (2003) 036706.
[23] X. He, G.D. Doolen, T. Clark, J. Comput. Phys. 179 (2002) 439.
[24] X. He, S. Chen, G.D. Doolen, J. Comput. Phys. 146 (1998) 282.